Combined Experimental-Simulation Based Acoustic Source Localization

Stefan Gombots[1], Manfred Kaltenbacher[1] and Barbara Kaltenbacher[2]
[1] Institute of Mechanics and Mechatronics, 1060 Vienna, Austria, Email: stefan.gombots@tuwien.ac.at
[2] Institute of Applied Analysis, 9020 Klagenfurt, Austria

Introduction

Acoustic source localization is a main task in the development of new products. In the last years, considerable improvements have been achieved in acoustic source localization using microphone arrays. However, main restrictions are given by simplified source models and describing the transfer function between source and microphone signal using Green's function for free radiation. Therefore, obstacles that prevent free radiation will not be appropriately taken into account by this description. Furthermore, reflecting (or partially reflecting) surfaces are not really considered, and the method of using mirror sources is quite limited. To overcome these limitations, we will combine measurement with simulation. The correct transfer function between source and microphone position will be determined by a finite element simulation (FE simulation). An alternative approach would be to solve the corresponding partial differential equation in the frequency domain (Helmholtz equation) with the actual boundary conditions as given in the measurement setup and solve the inverse problem of matching measured (microphone signals) and simulated pressure [1].
The applicability in real world situations and the additional benefit of our combined approach compared to standard beamforming will be demonstrated.

Theory

A often used method for acoustic source localization is beamforming, e. g. Standard Beamforming, Functional Beamforming [2], CLEAN [3], CLEANSC [4]. Beamforming is used to determine source locations and distributions, and to identify the source strength. In the following we consider beamforming just in the frequency domain. Therefore, the physical model is given by the Helmholtz equation

$$\Delta\hat{p}(\boldsymbol{x}) + k^2\hat{p}(\boldsymbol{x}) = \sigma\delta(\boldsymbol{x}) \tag{1}$$

with the wave number k. The boundary condition is given by the Sommerfeld's radiation condition

$$\lim_{r\to\infty} r^{\frac{n-1}{2}} \left(\frac{\partial\hat{p}}{\partial r} - jk\hat{p}\right) = 0 \tag{2}$$

with n the dimension of space and j the imaginary unit. We assume further that the original geometry of the setup and the Fourier-transformed pressure signals $p_{\mathrm{m},i}(\omega)$ (ω being the angular frequency, $i = 1, ..., M$) measured by microphones at position $\boldsymbol{x}_{\mathrm{m},i}$ are known. The acoustic sources in the beamforming algorithms are in most cases modelled by monopoles

$$\hat{p} = \sigma g_{\mathrm{free}}(r) \tag{3}$$

with the source strength σ and the Green's function for free radition $g_{\mathrm{free}}(r)$. In the 2 dimensional case the Green's function reads as

$$g_{\mathrm{2D}}(r) = \frac{j}{4}H_0^{(2)}(kr) \tag{4}$$

and in the 3 dimensional case

$$g_{\mathrm{3D}}(r) = \frac{1}{4\pi r}\, e^{-jkr} \tag{5}$$

with $r = |\boldsymbol{x}_{\mathrm{s}} - \boldsymbol{x}_{\mathrm{m},i}|$ the distance between source point $\boldsymbol{x}_{\mathrm{s}}$ and microphone position $\boldsymbol{x}_{\mathrm{m},i}$, and $H_0^{(2)}$ the Bessel function of third kind (Hankel function).

Standard Beamforming (StdBF)

The fundamental processing method in the frequency domain is StdBF, which is robust and fast. First, the cross spectral matrix (CSM) $\boldsymbol{C}$ is computed, out of the measured pressure amplitudes

$$\boldsymbol{C} = \hat{\boldsymbol{p}}\,\hat{\boldsymbol{p}}^{\mathrm{H}}, \tag{6}$$

where ^{H} denotes the hermitian operation (complex conjugation) and $\hat{\boldsymbol{p}}$ is the M-dimensional vector of the measured pressure. The modelled pressure is computed by (3). After minimization of the functional

$$J(a) = ||\boldsymbol{C} - a\boldsymbol{g}_{\mathrm{free}}\boldsymbol{g}_{\mathrm{free}}^{H}||^2, \tag{7}$$

we obtain the beamforming map

$$a = \frac{\boldsymbol{g}_{\mathrm{free}}^{\mathrm{H}}\boldsymbol{C}\boldsymbol{g}_{\mathrm{free}}}{\left(\boldsymbol{g}_{\mathrm{free}}^{\mathrm{H}}\boldsymbol{g}_{\mathrm{free}}\right)^2} \tag{8}$$

with $a = \sigma^2$. The process of determining the Green's function for the beamform map is illustrated in Fig. 1.

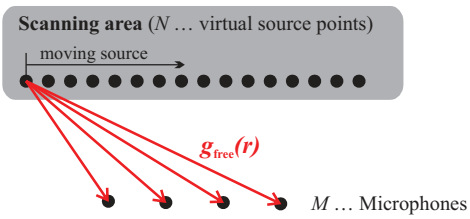

Figure 1: By moving the source over the predefined scanning area the Green's function for free radiation will be determined between the virtual source points and the microphone positions.

Beamforming with numerically calculated Green's function

As for StdBF, we compute in a first step the CSM (6). Now, the actual boundary conditions given by the measurement setup (e. q. obstacles and/or reflecting surfaces) will be considered by a FE simulation, and the numerical Green's function is obtained by

$$g_{\text{fem}}(r) = \frac{\hat{p}}{\sigma} \tag{9}$$

with $\sigma = 1$. Finally, the beamform map will be computed by

$$a = \frac{\boldsymbol{g}_{\text{fem}}^{\text{H}} \boldsymbol{C} \boldsymbol{g}_{\text{fem}}}{\left(\boldsymbol{g}_{\text{fem}}^{\text{H}} \boldsymbol{g}_{\text{fem}}\right)^2}. \tag{10}$$

The calculation of the Green's functions was modified compared to Fig. 1. Because of a reciprocal calculation (see Fig. 2), where the virtual source points are interchanged with the microphone positions, the number of calculations is minimized. By application of this methodology the number of FE simulations is reduced by $N - M$.

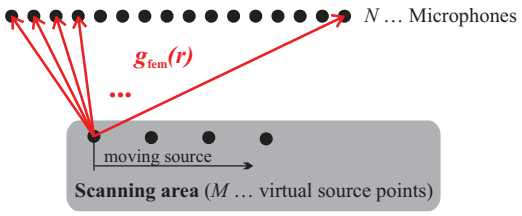

Figure 2: Illustration of the reciprocal calculation.

Comparison

To demonstrate the benefit of the numerically calculated Green's function, investigations were done with simulations in CFS++ [5]. First, in order to generate synthetic data, a FE simulation was performed and the CSM was calculated. This step provides virtually the measurement data as obtained by a microphone array. Next, the Green's functions for free radiation (see (4),(5)) between microphones and virtual source points were determined and furthermore the numerical Green's functions were calculated by FE simulations. With the CSM and the Green's functions the beamforming maps in the case of StdBf and Beamforming with numerically calculated Green's functions were determined. Last, both results were compared. The process is shown in Fig. 3.

Simulations

For the FE simulations a sound source described by

$$\sigma(x, y, t) = e^{-10^4 (x_q^2 + y_q^2)} \sin(2\pi f t) \tag{11}$$

was used, with frequency $f = 1000\,\text{Hz}$ and x_q, y_q the source coordinates. The simulations were made with two different types of microphone arrays:

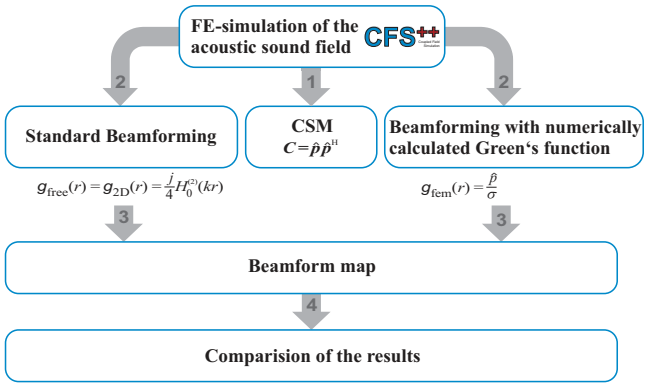

Figure 3: Process of the comparison of StdBF and Beamforming with numerical calculated Green's function.

- line array ($M = 15$, microphone spacing $\Delta = \lambda/4$)
- circle array ($M = 15$, radius $R = 2\lambda$)

with the wavelength λ.

Validation

First of all, simulations were made to validate the numerical method. Therefore the sound source was placed in an environment with no reflecting surfaces or obstacles. In Fig. 4, one can see the simulated acoustic field and the microphone positions. In this setup both methods of

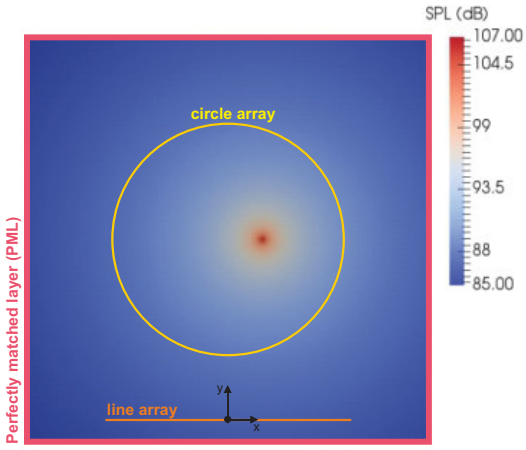

Figure 4: Setup to validate the numerical method, to guarantee free field conditions a perfectly matched layer was used. Source position $x_q = \lambda/2, y_q = 3\lambda$.

calculating the Green's function should produce the same beamforming map, as one can see in Fig. 5 and Fig. 6. The validation shows good agreement.

Reflecting surface

Beamforming is a method which mainly uses the phase information of the microphones to localize the acoustic sources. These informations can be corrupted amongst others through reflecting surfaces (e. g. floor, walls, ...). The enhancement, which can be achieved by a numerically calculated Green's function, is demonstrated by investigation of the given setup (Fig. 7). If the distance

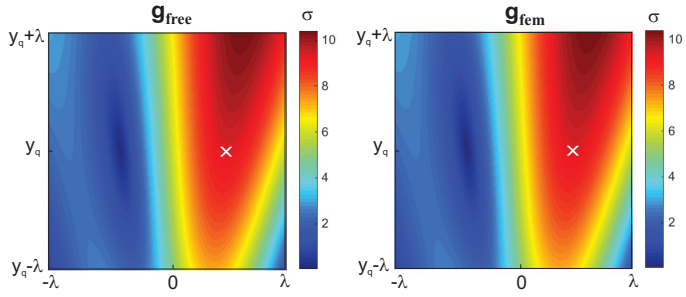

Figure 5: Line array - validation result. The white X indicates the correct source position.

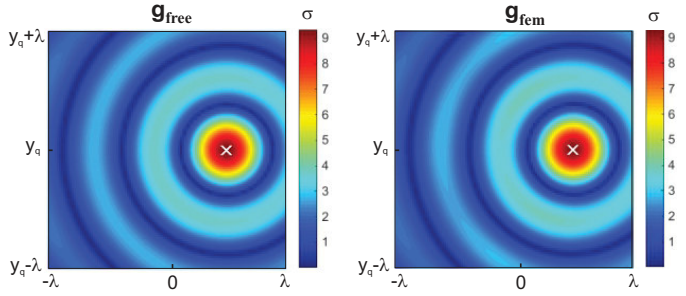

Figure 6: Circle array - validation result.

from microphone array to the source is given, the beamforming map in Fig. 8 shows a good localization result with a small error by using the numerically calculated Green's function and the source strength will by determined correctly. The Green's function for free radiation provides an bad localization result and the same applies to the source strength. Next, we will look at a scanning area. These beamforming maps (see Fig. 9) demonstrate the benefits of the numerically calculated Green's function best. The source position and the source strength are well reconstructed.

Obstacle

The free radiation can be disturbed by an obstacle. To illustrate the effect the setup in Fig. 10 was used. The dimensions of the acoustically hard obstacle and the microphone positions of the line and circle array can be seen in Fig. 10. First, we consider a scanning line which corresponds to the correct position of the placed sound source,

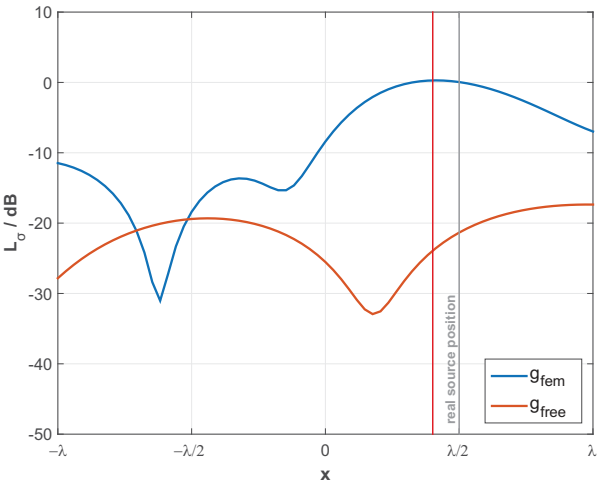

Figure 8: Beamforming map with correct focus to the source position. A small localization error occur (*red line*).

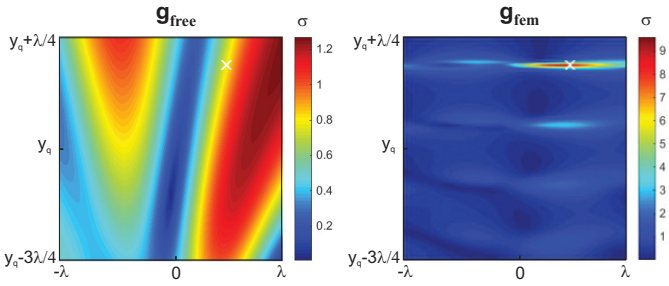

Figure 9: Reflecting surface in a distance of $\lambda/4$ from the source. The source was located at $x_q = \lambda/2, y_q = 3\lambda$.

no mismatch by focus. If the line array is used for determining the source location and strength, we get a very good result with the numerically calculated Green's function. By using the Green's function of free radiation we can identify the source but the resolution (beamwidth) is bad. The results with the circle array show similar quality of resolution, but here one can see that the sidelobe level improves approximetely from -10 dB to -20 dB. A comparison of the scanning line results of both array types can be seen in Fig. 11. The correct position of the sound source won't be known at beginning, therefore we will next use a scanning area to investigate the

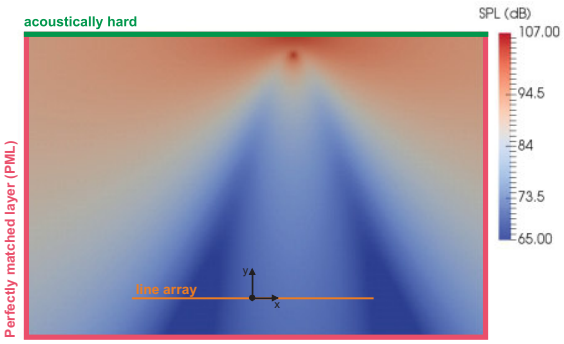

Figure 7: Reflecting surface in a distance of $\lambda/4$ from the source. The source was located at $x_q = \lambda/2, y_q = 3\lambda$.

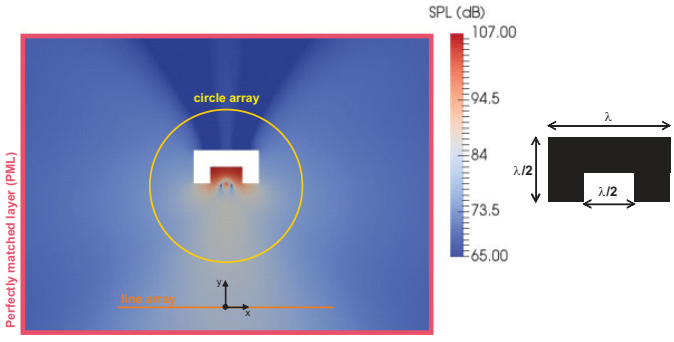

Figure 10: Simulation setup (*left*), source position $x_q = 0, y_q = 3\lambda$.; Dimensions of the obstacle (*right*).

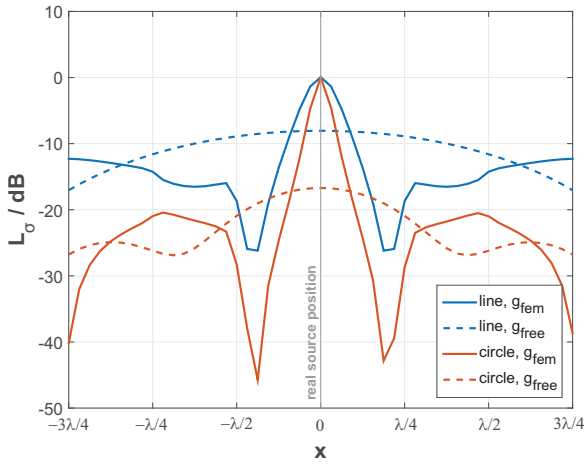

Figure 11: Beamform map of the line and circle array by applying the correct focus to the source position.

given setup. The beamforming maps produced by the line array (Fig. 12) shows the benefit of the numerically calculated Green's function, the position was not completely correctly reconstructed but the error is quite small (0.01 m in the y-direction). The results with the Green's function for free radiation do not identify the correct position. One can observe the typical behaviour of determining a too strong source strength, if the focus is larger than the correct distance (and vice versa). If

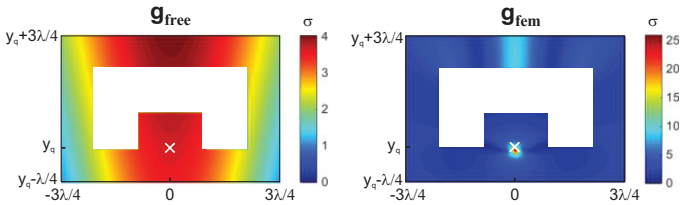

Figure 12: 2D beamform map of the line array.

we consider the beamforming maps from the circle array (Fig. 13) we get for both methods good results. Nevertheless the beamforming map of the calculated Green's function shows the better result of a smaller source localization result and also the reconstruction of the source strength is much better.

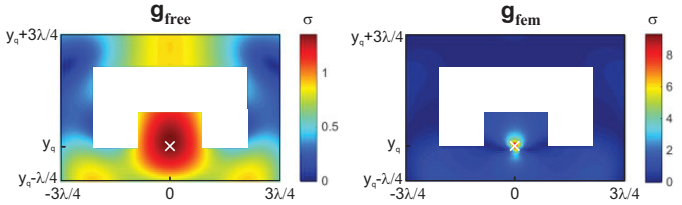

Figure 13: 2D beamform map of the circle array.

Conclusion

The influence of the main restrictions of beamforming, e. g. reflecting surfaces and obstacles can be minimized if the correct transfer function between source and microphone is known. Therefore, the transfer function (Green's function) was calculated by using a FE simulation with the actual boundary conditions as given. The investigations, which were made, show the improvements of identifying the sound source by the numerically calculated Green's function.

References

[1] Kaltenbacher, M., Kaltenbacher, B.: Inverse Scheme for Acoustic Source Localization based on Microphone Array Measurements, The 12th international Conference on Methematical and Numerical Aspects of Wave Propagation, 2015, p. 208-209

[2] Dougherty, R.: Functional Beamforming, 2014, BeBeC-2014-01

[3] Högborn, J.: Aperture Synthesis with a Non-Regular Distribution of Interferometer Baselines, 1974, Astronomy and Astrophysics Supplement, Vol. 15, p.417-426,

[4] Sijtsma, P.: Clean based on spatial source coherence, Int. J. Aeroacoustics 6, 2009, p. 357-374

[5] Kaltenbacher, M.: Numerical Simulation of Mechatronic Sensors and Actuators: Finite elements for Computational Multiphysics, 3rd Edition, Springer Verlag, 2015